International Journal of Control and Automation
Vol. 9, No. 6 (2016), pp.11-36
http//dx.doi.org/10.14257/ijca.2016.9.6.02

Design of a Model-Following Controller Using a Normalized Plant for SISO and MIMO

Shota Inoue[1] and Yoshihisa Ishida[2]

[1]Graduate School of Science and Technology, Meiji University, 1-1-1 Higashimita, Tamaku, Kawasaki, Kanagawa 214-8571, Japan
[2]School of Science and Technology, Meiji University, 1-1-1 Higashimita, Tamaku, Kawasaki, Kanagawa 214-8571, Japan
[1]ce41009@meiji.ac.jp, [2]ishida@meiji.ac.jp

Abstract

In this paper, we proposed a model-following controller for single-input-single-output (SISO) and multiple-input-multiple-output (MIMO) systems. This control system does not include plant parameters, and thus is designed using normalized plant. Moreover, we propose a design method of the normalized plant for the controlled plant with zero. And furthermore, we propose a design method for model-following controllers, which can easily decouple for MIMO systems. Simulation and experimental results show that the proposed method is robust to plant parameter variations and external disturbances.

***Keywords**: Model-Following Control, Normalized Plant, Robust Control, Decoupling*

1. Introduction

In industry, a model-following control is used when a control specification is imposed on the transient response characteristic to a reference input [1,2]. This system aims to make the plant output follow a desired reference model output. To prevent a steady-state error of the plant output even if a modeling error or a disturbance occurs in the controlled plant, integral compensation is required. A model-following servo system with integral compensation has been designed by stabilizing the expanded system with integral compensation for any deviation [3-8]. Nonami et al. proposed a model-following-type model predictive control as an extension of the pre-existing model predictive control (MPC) system [9,10]. The design method ensures robustness by considering an error that may occur in the future.

There are two problems with these model-following controller systems. First, because these controllers are designed using plant parameters, they have to be redesigned when the parameters change in a major way. Third, there are decoupling problems for MIMO systems. The decoupling problem gives a one-to-one correspondence between the input and the output. There are many reports about this problem, and basic important results are already known [11-14]. As a specific example, there are design methods based on state feedback [15] and using a state decoupler [16-18]. However, most of them depend on plant parameters.

On the other hand, a normalized plant was proposed as a design method that is independent of the plant parameters [19]. However, the normalized plant has been proposed only for SISO systems and has not been applied to model-following controller systems. Furthermore, there is no mention of the normalized plant for the controlled plant with zeros.

In this paper, a model-following controller is designed using a normalized plant for SISO and MIMO systems and is independent of plant parameters. In SISO system, the normalized plant is designed for the plant with zeros. In MIMO system, the designed

ISSN: 2005-4297 IJCA

method can easily decouple without using the state decoupler. The decoupling characteristic is improved by changing the magnitude of only one gain.

This paper is organized as follows. In Section 2, the structure of the normalized plants is described. In Section 3, the design methodology for the model-following controller proposed by Nonami et al. is described. In Section 4, the structure of the model-following controller using the normalized plants in the SISO and MIMO systems is described. In Section 5, the effectiveness of the proposed method is confirmed for several types of plants with simulation results. In Section 6, the effectiveness of the proposed method for a DC motor is confirmed by experimental results. Section 7 presents the conclusion.

2. Normalized Plants

2.1. SISO System

The transfer function of the controlled plant with zeros is described by

$$G(s)=\frac{Y(s)}{U(s)} = \frac{b_m s^{m-1}+b_{m-1}s^{m-2}+\cdots+b_2 s+b_1}{s^{n-1}+a_{n-1}s^{n-1}+\cdots+a_2 s+a_1}, \quad (1)$$

then the controlled plant is assumed as proper ($n \geq m$), and where $a_i\,(i=1,2,\cdots,n-1)$ and $b_j\,(j=1,2,\cdots,m)$ are plant parameters. Here, we insert an Integrator in front of the plant. The transfer function is obtained as

$$G(s)=\frac{Y(s)}{s^{m-1}U(s)} = \frac{b_m s^{m-1}+b_{m-1}s^{m-2}+\cdots+b_2 s+b_1}{a^{m-1}(s^{n-1}+a_{n-1}s^{n-1}+\cdots+a_2 s+a_1)}. \quad (2)$$

Equation (2) may also be described as

$$\dot{\boldsymbol{x}}(t)=\boldsymbol{A}_s\boldsymbol{x}(t)+\boldsymbol{B}_s u(t)^{(m-1)}, \quad (3a)$$

$$y(t)=\boldsymbol{C}_s\boldsymbol{x}(t), \quad (3b)$$

where,

$$\boldsymbol{x}(t)=\begin{bmatrix}\boldsymbol{x}_a(t)\\ \boldsymbol{u}(t)\end{bmatrix}\in\mathbb{R}^{\{(n-1)+(m-1)\}\times 1}, \boldsymbol{A}_s=\begin{bmatrix}\boldsymbol{A}_a & \boldsymbol{B}_a\\ \boldsymbol{0} & \boldsymbol{\Omega}\end{bmatrix}\in\mathbb{R}^{\{(n-1)+(m-1)\}\times\{(n-1)+(m-1)\}},$$

$$\boldsymbol{B}_s=\begin{bmatrix}\boldsymbol{B}_b\\ \boldsymbol{\Theta}\end{bmatrix}\in\mathbb{R}^{\{(n-1)+(m-1)\}\times 1}, \boldsymbol{C}_s=\begin{bmatrix}\boldsymbol{C}_a\\ \boldsymbol{0}\end{bmatrix}\in\mathbb{R}^{1\times\{(n-1)+(m-1)\}}.$$

Hence, $\boldsymbol{x}_a(t)\in^{(n-1)\times 1}$, $\boldsymbol{u}(t)\in\mathbb{R}^{(m-1)\times 1}$, $\boldsymbol{A}_a\in\mathbb{R}^{(n-1)\times(n-1)}$, $\boldsymbol{B}_a\in\mathbb{R}^{(n-1)\times(m-1)}$, $\boldsymbol{\Omega}\in\mathbb{R}^{(m-1)\times(m-1)}$, $\boldsymbol{B}_b\in\mathbb{R}^{(n-1)\times 1}$, $\boldsymbol{\Theta}\in\mathbb{R}^{(m-1)\times 1}$, and $\boldsymbol{C}_a\in\mathbb{R}^{1\times(n-1)}$ are described by

$$\boldsymbol{x}(t)=\begin{bmatrix}x_1(t)\\ x_2(t)\\ \vdots\\ x_{n-2}(t)\\ x_{n-1}(t)\end{bmatrix}, \boldsymbol{u}(t)=\begin{bmatrix}u(t)\\ \dot{u}(t)\\ \vdots\\ u(t)^{(m-3)}\\ u(t)^{(m-2)}\end{bmatrix},$$

$$\boldsymbol{A}_a=\begin{bmatrix}0 & 1 & 0 & \cdots & 0\\ 0 & 0 & 1 & \ddots & \vdots\\ \vdots & \ddots & \ddots & \ddots & 0\\ 0 & \cdots & \cdots & 0 & 1\\ -a_1 & -a_2 & \cdots & -a_{n-2} & -a_{n-1}\end{bmatrix},$$

$$\boldsymbol{B}_b=\begin{bmatrix}0\\ 0\\ \vdots\\ 0\\ b_m\end{bmatrix},\boldsymbol{\Theta}=\begin{bmatrix}0\\ 0\\ \vdots\\ 0\\ 1\end{bmatrix},\boldsymbol{C}_a=\begin{bmatrix}1\\ 0\\ \vdots\\ 0\\ 0\end{bmatrix}^{\mathrm{T}},$$

$$\boldsymbol{B}_a=\begin{bmatrix}0 & 0 & \cdots & 0 & 0\\ 0 & 0 & \cdots & 0 & 0\\ \vdots & \vdots & \ddots & \vdots & \vdots\\ 0 & 0 & \cdots & 0 & 0\\ b_1 & b_2 & \cdots & b_{m-2} & b_{m-1}\end{bmatrix},\boldsymbol{\Omega}=\begin{bmatrix}0 & 1 & 0 & \cdots & 0\\ 0 & 0 & 1 & \ddots & \vdots\\ \vdots & \vdots & \ddots & \ddots & 0\\ 0 & 0 & \cdots & 0 & 1\\ 0 & 0 & \cdots & \cdots & 0\end{bmatrix},$$

$$\boldsymbol{B}_b=\begin{bmatrix}0\\ 0\\ \vdots\\ 0\\ b_m\end{bmatrix},\boldsymbol{\Theta}=\begin{bmatrix}0\\ 0\\ \vdots\\ 0\\ 1\end{bmatrix},\boldsymbol{C}_a=\begin{bmatrix}1\\ 0\\ \vdots\\ 0\\ 0\end{bmatrix}^{\mathrm{T}}.$$

Then, the normalized plant [19] is adopted for the system of (3). As shown in Figure 1, the manipulated variable is given by

$$u(t)=\frac{1}{b_m}(v_n(t)-\boldsymbol{A}_u\boldsymbol{x}(t)), \tag{4}$$

where

$$\boldsymbol{A}_u=\begin{bmatrix}-a_1 & -a_2 & \cdots & -a_{n-2} & -a_{n-1} & b_1 & b_2 & \cdots & b_{m-2} & b_{m-1}\end{bmatrix},$$

and $v_n(t)$ is a new manipulated variable. By substituting Eq. (4) into Eq. (3a), the following equations are obtained:

$$\begin{aligned}\dot{\boldsymbol{x}}(t)&=\boldsymbol{A}_s\boldsymbol{x}(t)+\boldsymbol{B}\frac{1}{b_m}(v_n(t)-\boldsymbol{A}_u\boldsymbol{x}(t))\\ &=\boldsymbol{A}_s\boldsymbol{x}(t)+\frac{1}{b_m}\boldsymbol{B}v_n(t)-\frac{1}{b_m}\boldsymbol{B}\boldsymbol{A}_u\boldsymbol{x}(t)\\ &=\left(\boldsymbol{A}_s-\frac{1}{b_m}\boldsymbol{B}\boldsymbol{A}_u\right)\boldsymbol{x}(t)+\frac{1}{b_m}\boldsymbol{B}v_n(t)\\ &=\bar{\boldsymbol{A}}\boldsymbol{x}(t)+\bar{\boldsymbol{B}}v_n(t), \qquad (5a)\\ y(t)&=\bar{\boldsymbol{C}}\boldsymbol{x}(t), \qquad (5b)\end{aligned}$$

where

$$\bar{\boldsymbol{A}} = \begin{bmatrix} \tilde{\boldsymbol{A}} & \boldsymbol{0} \\ \bar{\boldsymbol{A}}_a & \bar{\boldsymbol{B}}_a \end{bmatrix} \in \mathbb{R}^{\{(m-1)+(n-1)\}\times\{(m-1)+(n-1)\}},$$

$$\bar{\boldsymbol{B}} = \begin{bmatrix} \boldsymbol{\psi} \\ \bar{\boldsymbol{B}}_b \end{bmatrix} \in \mathbb{R}^{\{(m-1)+(n-1)\}\times 1}, \bar{\boldsymbol{C}} = \begin{bmatrix} \boldsymbol{C}_a \\ \boldsymbol{0} \end{bmatrix}^{\mathrm{T}} \in \mathbb{R}^{1\times\{(m-1)+(n-1)\}},$$

Hence, $\tilde{\boldsymbol{A}}$, $\bar{\boldsymbol{A}}_a$, $\bar{\boldsymbol{B}}_a$, $\boldsymbol{\Psi}$, $\bar{\boldsymbol{B}}_b$ are described by

$$\tilde{\boldsymbol{A}} = \begin{bmatrix} 0 & 1 & 0 & \cdots & 0 \\ 0 & 0 & 1 & \ddots & \vdots \\ \vdots & \vdots & \vdots & \ddots & 0 \\ 0 & 0 & 0 & \cdots & 1 \\ 0 & 0 & 0 & \cdots & 0 \end{bmatrix}, \bar{\boldsymbol{A}}_a = \begin{bmatrix} 0 & 0 & 0 & \cdots & 0 \\ 0 & 0 & 0 & \ddots & \vdots \\ \vdots & \vdots & \vdots & \ddots & 0 \\ 0 & 0 & 0 & \cdots & 0 \\ \frac{a_1}{b_m} & \frac{a_2}{b_m} & \frac{a_3}{b_m} & \cdots & \frac{a_{n-1}}{b_m} \end{bmatrix}$$

$$\bar{\boldsymbol{B}}_a = \begin{bmatrix} 0 & 1 & 0 & \cdots & 0 \\ 0 & 0 & 1 & \ddots & \vdots \\ \vdots & & \ddots & \ddots & 0 \\ 0 & \cdots & \cdots & 0 & 1 \\ \frac{b_1}{b_m} & \frac{b_2}{b_m} & \frac{b_3}{b_m} & \cdots & \frac{b_{m-1}}{b_m} \end{bmatrix}, \boldsymbol{\psi} = \begin{bmatrix} 0 \\ 0 \\ \vdots \\ 0 \\ 1 \end{bmatrix}, \bar{\boldsymbol{B}}_b = \begin{bmatrix} 0 \\ 0 \\ \vdots \\ 0 \\ \frac{1}{b_m} \end{bmatrix}.$$

The controlled system is described by (5). Here, the transfer function is rewritten as (5) from (1):

$$G(s) = \bar{\boldsymbol{C}}(s\boldsymbol{I} - \bar{\boldsymbol{A}})^{-1}\bar{\boldsymbol{B}} = \frac{1}{s^{n-1}}. \tag{6}$$

Therefore, the controlled system is described by (6) and does not include plant parameters:

$$\dot{\boldsymbol{x}}(t) = \tilde{\boldsymbol{A}}\boldsymbol{x}(t) + \tilde{\boldsymbol{B}}v(t), \tag{7a}$$

$$y(t) = \tilde{\boldsymbol{C}}\boldsymbol{x}(t), \tag{7b}$$

where

$$\bar{\boldsymbol{A}} = \begin{bmatrix} 0 & 1 & 0 & \cdots & 0 \\ 0 & 0 & 1 & \ddots & \vdots \\ \vdots & & \ddots & \ddots & 0 \\ 0 & \cdots & \cdots & 0 & 1 \\ 0 & 0 & \cdots & 0 & 0 \end{bmatrix}, \bar{\boldsymbol{B}} = \begin{bmatrix} 0 \\ 0 \\ \vdots \\ 0 \\ 1 \end{bmatrix}, \bar{\boldsymbol{C}} = \begin{bmatrix} 1 \\ 0 \\ \vdots \\ 0 \\ 0 \end{bmatrix}^{\mathrm{T}}.$$

Equation. (7) describes a normalized plant of the controlled plant with zeros for a SISO system. The block diagram of the normalized plant is shown in Figure 2.

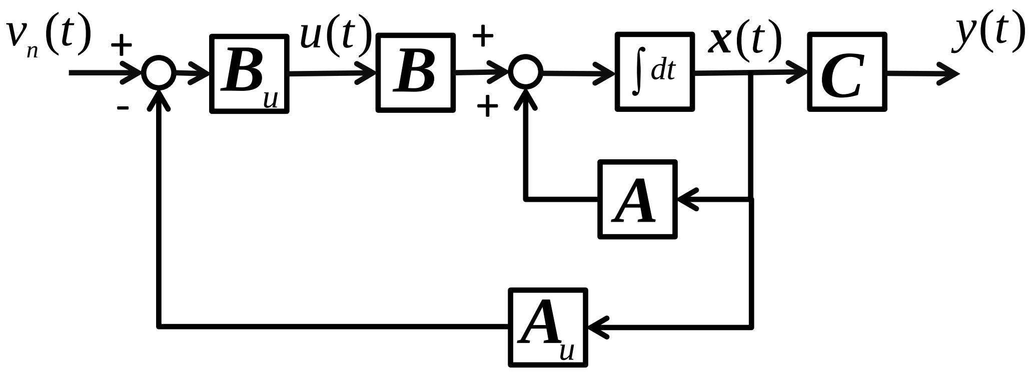

Figure 1. Structure of the Normalized Plant

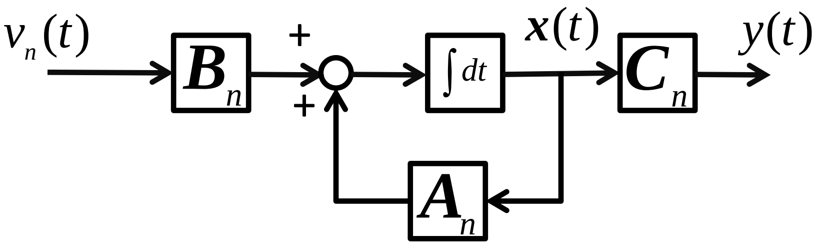

Figure 2. The Normalized Plant

2.1. MIMO System

In this section, the proposed method for the normalized plant for MIMO system. Let the state-space plant model of the n-th degree of the p-input q-output be:

$$\dot{\boldsymbol{x}}(t) = \boldsymbol{A}\boldsymbol{x}(t) + \boldsymbol{B}u(t), \tag{8a}$$

$$y(t) = \boldsymbol{C}\boldsymbol{x}(t), \tag{8b}$$

where $\boldsymbol{A}$, $\boldsymbol{B}$, and $\boldsymbol{C}$ are

$$\boldsymbol{A} = \begin{bmatrix} \boldsymbol{A}_{11} & \boldsymbol{A}_{12} & \cdots & \boldsymbol{A}_{1k} \\ \boldsymbol{A}_{21} & \boldsymbol{A}_{22} & \cdots & \boldsymbol{A}_{2k} \\ \vdots & \vdots & \ddots & \vdots \\ \boldsymbol{A}_{k1} & \boldsymbol{A}_{k2} & \cdots & \boldsymbol{A}_{kk} \end{bmatrix}, \boldsymbol{B} = \begin{bmatrix} \boldsymbol{B}_{11} & \boldsymbol{B}_{12} & \cdots & \boldsymbol{B}_{1p} \\ \boldsymbol{B}_{21} & \boldsymbol{B}_{22} & \cdots & \boldsymbol{B}_{2p} \\ \vdots & \vdots & \ddots & \vdots \\ \boldsymbol{B}_{k1} & \boldsymbol{B}_{k2} & \cdots & \boldsymbol{B}_{kp} \end{bmatrix},$$

$$\boldsymbol{C} = \begin{bmatrix} \boldsymbol{C}_{11} & \boldsymbol{C}_{12} & \cdots & \boldsymbol{C}_{1k} \\ \boldsymbol{C}_{21} & \boldsymbol{C}_{22} & \cdots & \boldsymbol{C}_{2k} \\ \vdots & \vdots & \ddots & \vdots \\ \boldsymbol{C}_{q1} & \boldsymbol{C}_{q2} & \cdots & \boldsymbol{C}_{qk} \end{bmatrix},$$

where the degree n of the system is $n = l \times k$, and $\boldsymbol{A}_{ij} \in \mathbb{R}^{l \times l}$, $\boldsymbol{B}_{ij} \in \mathbb{R}^{l \times 1}$, and $\boldsymbol{C}_{ij} \in \mathbb{R}^{1 \times l}$ are described by the following:

$$\boldsymbol{A}_{ij}\begin{cases}=\begin{bmatrix}0 & 1 & 0 & \cdots & 0\\ \vdots & 0 & 1 & \ddots & \vdots\\ \vdots & & \ddots & \ddots & 0\\ 0 & \cdots & \cdots & 0 & 1\\ a_{ij,1} & a_{ij,2} & \cdots & a_{ij,l-1} & a_{ij,l}\end{bmatrix} & (i=j)\\ =\begin{bmatrix}0 & 0 & 0 & \cdots & 0\\ \vdots & 0 & 0 & \ddots & \vdots\\ \vdots & & \ddots & \ddots & 0\\ 0 & \cdots & \cdots & 0 & 0\\ a_{ij,1} & a_{ij,2} & \cdots & a_{ij,l-1} & a_{ij,l}\end{bmatrix} & (i\neq j)\end{cases},$$

$$\boldsymbol{B}_{ij}\begin{cases}=\begin{bmatrix}0 & \cdots & 0 & b_{ij}\end{bmatrix}^T & (i=j)\\ =\begin{bmatrix}0 & 0 & \cdots & \hat{b}_{ij}\end{bmatrix}^T & (i\neq j)\end{cases},$$

$$\boldsymbol{C}_{ij}\begin{cases}=\begin{bmatrix}1 & 0 & \cdots & 0\end{bmatrix} & (i=j)\\ =\begin{bmatrix}0 & 0 & \cdots & 0\end{bmatrix} & (i\neq j)\end{cases},$$

for $i, j=1,2,\cdots,n$. In particular, when $i\neq j$ and $a_{ij,l}=\hat{b}_{ij}=0$, Eq. (8) is called a decoupled plant. Generally, the following inequality is satisfied:

$$b_{ij} \gg \hat{b}_{ij}. \tag{9}$$

From Eq. (4), the manipulated variable for MIMO systems is given as follows:

$$\boldsymbol{u}(t)=\boldsymbol{B}_u(\boldsymbol{v}_n(t)-\boldsymbol{A}_u\boldsymbol{x}(t)), \tag{10}$$

where $\boldsymbol{v}_n \in \mathbb{R}^p$ is a new manipulated variable and the matrices $\boldsymbol{A}_u$ and $\boldsymbol{B}_u$ are given by the following matrices:

$$\boldsymbol{A}_u=\begin{bmatrix}\tilde{\boldsymbol{A}}_{11} & \tilde{\boldsymbol{A}}_{12} & \cdots & \tilde{\boldsymbol{A}}_{1k}\\ \tilde{\boldsymbol{A}}_{21} & \tilde{\boldsymbol{A}}_{22} & \cdots & \tilde{\boldsymbol{A}}_{2k}\\ \vdots & \vdots & \ddots & \vdots\\ \tilde{\boldsymbol{A}}_{k1} & \tilde{\boldsymbol{A}}_{k2} & \cdots & \tilde{\boldsymbol{A}}_{kk}\end{bmatrix}, \boldsymbol{B}_u=\begin{bmatrix}1/b_{11} & 0 & \cdots & 0\\ 0 & 1/b_{22} & \ddots & \vdots\\ \vdots & \ddots & \ddots & 0\\ 0 & \cdots & 0 & 1/b_{pp}\end{bmatrix},$$

$$\tilde{\boldsymbol{A}}_{ij}\begin{cases}=\begin{bmatrix}a_{ij,1} & a_{ij,2} & \cdots & a_{ij,l-1} & a_{ij,l}\end{bmatrix}\in\mathbb{R}^{1\times l} & (i=j)\\ =\begin{bmatrix}0 & 0 & \cdots & 0 & 0\end{bmatrix}\in\mathbb{R}^{1\times l} & (i\neq j)\end{cases}.$$

By substituting Eq. (10) into Eq. (8), the following equation can be obtained:

$$\begin{aligned}\dot{\boldsymbol{x}}(t)&=\boldsymbol{A}\boldsymbol{x}(t)+\boldsymbol{B}\boldsymbol{u}(t)\\ &=\boldsymbol{A}\boldsymbol{x}(t)+\boldsymbol{B}\left(\boldsymbol{B}_u(\boldsymbol{v}_n(t)-\boldsymbol{A}_u\boldsymbol{x}(t))\right)\\ &=\left(\boldsymbol{A}-\boldsymbol{B}\boldsymbol{B}_u\boldsymbol{A}_u\right)\boldsymbol{x}(t)+\boldsymbol{B}\boldsymbol{B}_u\boldsymbol{v}_n(t),\end{aligned} \tag{11}$$

where, considering Eq. (11), $\boldsymbol{B}\boldsymbol{B}_u$ is

$$\boldsymbol{B}\boldsymbol{B}_u \cong \begin{bmatrix} \tilde{\boldsymbol{B}}_{11} & \tilde{\boldsymbol{B}}_{12} & \cdots & \tilde{\boldsymbol{B}}_{1q} \\ \tilde{\boldsymbol{B}}_{21} & \tilde{\boldsymbol{B}}_{22} & \cdots & \tilde{\boldsymbol{B}}_{2q} \\ \vdots & \vdots & \ddots & \vdots \\ \tilde{\boldsymbol{B}}_{k1} & \tilde{\boldsymbol{B}}_{k2} & \cdots & \tilde{\boldsymbol{B}}_{kq} \end{bmatrix},$$

$$\tilde{\boldsymbol{B}}_{ij} \begin{cases} = \begin{bmatrix} 0 & \cdots & 0 & 1 \end{bmatrix}^T \in \mathbb{R}^{l\times 1} & (i=j) \\ = \begin{bmatrix} 0 & 0 & \cdots & 0 \end{bmatrix}^T \in \mathbb{R}^{l\times 1} & (i\neq j) \end{cases}.$$

Hence, Eq. (11) is described by

$$\dot{\boldsymbol{x}}(t) = \boldsymbol{A}_n \boldsymbol{x}(t) + \boldsymbol{B}_n \boldsymbol{v}_n(t), \tag{12}$$

where

$$\boldsymbol{A}_n = \begin{bmatrix} \bar{\boldsymbol{A}}_{11} & \bar{\boldsymbol{A}}_{12} & \cdots & \bar{\boldsymbol{A}}_{1k} \\ \bar{\boldsymbol{A}}_{21} & \bar{\boldsymbol{A}}_{22} & \cdots & \bar{\boldsymbol{A}}_{2k} \\ \vdots & \vdots & \ddots & \vdots \\ \bar{\boldsymbol{A}}_{k1} & \bar{\boldsymbol{A}}_{k2} & \cdots & \bar{\boldsymbol{A}}_{kk} \end{bmatrix}, \boldsymbol{B}_n = \begin{bmatrix} \bar{\boldsymbol{B}}_{11} & \bar{\boldsymbol{B}}_{12} & \cdots & \bar{\boldsymbol{B}}_{1p} \\ \bar{\boldsymbol{B}}_{21} & \bar{\boldsymbol{B}}_{22} & \cdots & \bar{\boldsymbol{B}}_{2p} \\ \vdots & \vdots & \ddots & \vdots \\ \bar{\boldsymbol{B}}_{k1} & \bar{\boldsymbol{B}}_{k2} & \cdots & \bar{\boldsymbol{B}}_{kp} \end{bmatrix},$$

$$\bar{\boldsymbol{A}}_{ij} \begin{cases} = \begin{bmatrix} 0 & 1 & 0 & \cdots & 0 \\ \vdots & 0 & 1 & \ddots & \vdots \\ \vdots & & \ddots & \ddots & 0 \\ 0 & \cdots & \cdots & 0 & 1 \\ 0 & 0 & \cdots & 0 & 0 \end{bmatrix} \in \mathbb{R}^{l\times l} & (i=j) \\ = \begin{bmatrix} 0 & 0 & 0 & \cdots & 0 \\ \vdots & 0 & 0 & \ddots & \vdots \\ \vdots & & \ddots & \ddots & 0 \\ 0 & \cdots & \cdots & 0 & 0 \\ 0 & 0 & \cdots & 0 & 0 \end{bmatrix} \in \mathbb{R}^{l\times l} & (i\neq j) \end{cases},$$

$$\bar{\boldsymbol{B}}_{ij} \begin{cases} = \begin{bmatrix} 0 & \cdots & 0 & 1 \end{bmatrix}^T \in \mathbb{R}^{l\times 1} & (i=j) \\ = \begin{bmatrix} 0 & 0 & \cdots & 0 \end{bmatrix}^T \in \mathbb{R}^{l\times 1} & (i\neq j) \end{cases}.$$

Equation. (12) is a normalized plant for MIMO systems. The block diagram of the normalized plant is about the same as that shown in Figure 2.

3. Model-Following Control

In this section, the conventional method for model-following control systems is explained [10].

Let the state-space model be as follows:

$$\dot{\boldsymbol{x}}_m(t) = \boldsymbol{A}_m \boldsymbol{x}_m(t) + \boldsymbol{B}_m \boldsymbol{r}(t), \tag{13a}$$

$$\boldsymbol{y}_m(t) = \boldsymbol{C}_m \boldsymbol{x}_m(t), \tag{13b}$$

where $\boldsymbol{x}_m(t) \in \mathbb{R}^{n\times 1}$ is the state vector of the model, $\boldsymbol{r}(t) \in \mathbb{R}^{p\times 1}$ is the model input, $\boldsymbol{y}_m(t) \in \mathbb{R}^{q\times 1}$ is the model output, $\boldsymbol{A}_m \in \mathbb{R}^{n\times n}$, $\boldsymbol{B}_m \in \mathbb{R}^{n\times p}$, and $\boldsymbol{C}_m \in \mathbb{R}^{q\times n}$ are the constant matrices of appropriate dimensions, and $\boldsymbol{C}_m = \boldsymbol{C}$. By denoting the error as $\boldsymbol{e}(t) = \boldsymbol{x}(t) - \boldsymbol{x}_m(t)$, the following equation can be obtained by subtracting Eq. (13a) from Eq. (8a):

$$\begin{aligned}\dot{\boldsymbol{e}}(t) &= \dot{\boldsymbol{x}}(t) - \dot{\boldsymbol{x}}_m(t) \\ &= \boldsymbol{A}\boldsymbol{x}(t) + \boldsymbol{B}u(t) - \boldsymbol{A}_m\boldsymbol{x}_m(t) - \boldsymbol{B}_m\boldsymbol{r}(t) \\ &= \boldsymbol{A}_m\left(\boldsymbol{x}(t) - \boldsymbol{x}_m(t)\right) - \boldsymbol{A}_m\boldsymbol{x}(t) + \boldsymbol{A}\boldsymbol{x}(t) + \boldsymbol{B}\boldsymbol{u}(t) - \boldsymbol{B}_m\boldsymbol{r}(t) \\ &= \boldsymbol{A}_m\boldsymbol{e}(t) + \left(\boldsymbol{A} - \boldsymbol{A}_m\right)\boldsymbol{x}(t) + \boldsymbol{B}\boldsymbol{u}(t) - \boldsymbol{B}_m\boldsymbol{r}(t).\end{aligned} \tag{14}$$

It is assumed that Eq. (14) satisfies the following model matching condition [10]:

$$\boldsymbol{A}_m - \boldsymbol{A} = \boldsymbol{B}\boldsymbol{K}_{1a},\ \boldsymbol{B}_m = \boldsymbol{B}\boldsymbol{K}_{2a}, \tag{15}$$

where $\boldsymbol{K}_{1a}$ is the feedback gain and $\boldsymbol{K}_{2a}$ is the feedforward gain. By substituting Eq. (15) into Eq. (14), the following is obtaine:

$$\dot{\boldsymbol{e}}(t) = \boldsymbol{A}_m\boldsymbol{e}(t) - \boldsymbol{B}\left(\boldsymbol{K}_{1a}\boldsymbol{x}(t) + \boldsymbol{K}_{2a}\boldsymbol{r}(t) - \boldsymbol{u}(t)\right). \tag{16}$$

The gains $\boldsymbol{K}_{1a}$ and $\boldsymbol{K}_{2a}$ are given by the following:

$$\begin{cases}\boldsymbol{K}_{1a} = \boldsymbol{B}^{+}\left(\boldsymbol{A}_m - \boldsymbol{A}\right) & (17) \\ \boldsymbol{K}_{2a} = \left(-\boldsymbol{C}_m\boldsymbol{A}_m^{-1}\boldsymbol{B}\right)^{-1}, & (18)\end{cases}$$

where $\boldsymbol{B}^{+}$ is the Moore–Penrose Matrix Inverse of $\boldsymbol{B}$. Let the plant input $\boldsymbol{u}(t)$ be

$$\boldsymbol{u}(t) = \boldsymbol{K}_{1a}\boldsymbol{x}(t) + \boldsymbol{K}_{2a}\boldsymbol{r}(t) + \boldsymbol{v}(t). \tag{19}$$

Then, the error $\boldsymbol{e}(t)$ is rewritten as follows:

$$\begin{aligned}\dot{\boldsymbol{e}}(t) &= \boldsymbol{A}_m\boldsymbol{e}(t) - \boldsymbol{B}\left(\boldsymbol{K}_{1a}\boldsymbol{x}(t) + \boldsymbol{K}_{2a}\boldsymbol{r}(t) - \boldsymbol{K}_{1a}\boldsymbol{x}(t) - \boldsymbol{K}_{2a}\boldsymbol{r}(t) - \boldsymbol{v}(t)\right) \\ &= \boldsymbol{A}_m\boldsymbol{e}(t) + \boldsymbol{B}\boldsymbol{v}(t).\end{aligned} \tag{20}$$

Meanwhile, the integral $\varepsilon(t)$ of the output deviation is

$$\begin{aligned}\dot{\varepsilon}(t) &= \boldsymbol{y}(t) - \boldsymbol{y}_m(t) \\ &= \boldsymbol{C}\boldsymbol{x}(t) - \boldsymbol{C}_m\boldsymbol{x}_m(t) \\ &= \boldsymbol{C}_m\boldsymbol{e}(t).\end{aligned} \tag{21}$$

The augmented system is derived from Eqs. (20) and (21) as follows:

$$\dot{\hat{\boldsymbol{e}}}(t) = \boldsymbol{A}_e\hat{\boldsymbol{e}}(t) + \boldsymbol{B}_e\boldsymbol{v}(t), \tag{22}$$

where

$$\boldsymbol{A}_e = \begin{bmatrix}\boldsymbol{A}_m & \boldsymbol{0} \\ \boldsymbol{C}_m & \boldsymbol{0}\end{bmatrix},$$

$$\boldsymbol{B}_e = \begin{bmatrix}\boldsymbol{B} \\ \boldsymbol{0}\end{bmatrix}, \hat{\boldsymbol{e}}(t) = \begin{bmatrix}\boldsymbol{e}(t) \\ \varepsilon(t)\end{bmatrix}.$$

The feedback gains $\boldsymbol{F}_{1a} \in \mathbb{R}^{p\times n}$ and $\boldsymbol{F}_{2a} \in \mathbb{R}^{q\times q}$ are obtained by minimizing the following evaluation function

$$J = \int_0^{\infty}\{\boldsymbol{e}'(t)^{\mathrm{T}}\boldsymbol{Q}\boldsymbol{e}'(t) + \boldsymbol{v}(t)^{\mathrm{T}}\boldsymbol{R}\boldsymbol{v}(t)\}dt, \tag{23}$$

where $\boldsymbol{Q} \in \mathbb{R}^{(n+q)\times(n+q)}$ is a diagonal matrix with positive elements ($\boldsymbol{Q} \geq 0$), and $\boldsymbol{R} \in \mathbb{R}^{p\times p}$ is a positive definite matrix ($\boldsymbol{R} > 0$). The optimal control gain, $\boldsymbol{K}_e = \left[\boldsymbol{F}_{1a} \quad \boldsymbol{F}_{2a}\right]$, that minimizes Eq. (23) is given as follows:

$$\boldsymbol{K}_e = -\boldsymbol{R}^{-1}\boldsymbol{B}_e\boldsymbol{P}. \tag{24}$$

The matrix $\boldsymbol{P}$ is the solution of the following Riccati equation:

$$\boldsymbol{P}\boldsymbol{A}_e + \boldsymbol{A}_e^{T}\boldsymbol{P} - \boldsymbol{P}\boldsymbol{B}_e\boldsymbol{R}^{-1}\boldsymbol{B}_e^{T}\boldsymbol{P} + \boldsymbol{Q} = \boldsymbol{0}. \tag{25}$$

Thus, $\boldsymbol{v}(t)$ is given by

$$\boldsymbol{v}(t) = \boldsymbol{F}_{1a}\boldsymbol{e}(t) + \boldsymbol{F}_{2a}\int\left(\boldsymbol{y}(t) - \boldsymbol{y}_m(t)\right)dt. \tag{26}$$

From Eqs. (19) and (26), the plant input $\boldsymbol{u}(t)$ is given as follows:

$$\boldsymbol{u}(t) = \boldsymbol{K}_{1a}\boldsymbol{x}(t) + \boldsymbol{K}_{2a}\boldsymbol{r}(t) + \boldsymbol{F}_{1a}\boldsymbol{e}(t) + \boldsymbol{F}_{2a}\int\left(\boldsymbol{y}(t) - \boldsymbol{y}_m(t)\right)dt. \tag{27}$$

4. Model-Following Control with Normalized Plants

This section describes the model-following control for the normalized plants.

4.1. SISO System

In Eq. (13), the matrices $\boldsymbol{A}_m$, $\boldsymbol{B}_m$, and $\boldsymbol{C}_m$ are defined as follows:

$$\boldsymbol{A}_m = \begin{bmatrix} 0 & 1 & 0 & \cdots & 0 \\ 0 & 0 & 1 & \ddots & \vdots \\ \vdots & \vdots & \ddots & \ddots & 0 \\ 0 & 0 & \cdots & 0 & 1 \\ -a_{m0} & -a_{m1} & \cdots & -a_{m(n-2)} & -a_{m(n-1)} \end{bmatrix} \in \mathbb{R}^{n\times n},$$

$$\boldsymbol{B}_m = \begin{bmatrix} 0 \\ \vdots \\ \vdots \\ 0 \\ b_m \end{bmatrix} \in \mathbb{R}^{n\times 1}, \boldsymbol{C}_m = \begin{bmatrix} 1 \\ 0 \\ \vdots \\ \vdots \\ 0 \end{bmatrix}^T \in \mathbb{R}^{1\times n}.$$

To apply the model-following control described in Section 2 to the normalized SISO plant, Eqs. (17) and (18) are given as follows:

$$\begin{aligned} \boldsymbol{K}_{1b} &= \boldsymbol{B}_n^{+}\left(\boldsymbol{A}_m - \boldsymbol{A}_n\right) \\ &= \begin{bmatrix} -a_{m0} & -a_{m1} & \cdots & -a_{m(n-2)} & -a_{m(n-1)} \end{bmatrix}, \end{aligned} \tag{28}$$

and

$$\begin{aligned} \boldsymbol{K}_{2b} &= \left(-\boldsymbol{C}_m\boldsymbol{A}_m^{-1}\boldsymbol{B}_n\right)^{-1} \\ &= -a_{m0}. \end{aligned} \tag{29}$$

Equations. (28) and (29) are determined only by model parameters.Let the plant input $u(t)$ be

$$u(t) = \boldsymbol{K}_{1b}\boldsymbol{x}(t) + \boldsymbol{K}_{2b}r(t) + \boldsymbol{B}_f v(t), \tag{30}$$

where

$$\boldsymbol{B}_f = \boldsymbol{B}^{+}{}_n\boldsymbol{B}_m. \tag{31}$$

Then, Eq. (20) can be rewritten as follows:

$$\begin{aligned} \dot{\boldsymbol{e}}(t) &= \boldsymbol{A}_m\boldsymbol{e}(t) - \boldsymbol{B}_n\left(\boldsymbol{K}_{1b}\boldsymbol{x}(t) + \boldsymbol{K}_{2b}r(t) - \boldsymbol{K}_{1b}\boldsymbol{x}(t) - \boldsymbol{K}_{2b}r(t) - \boldsymbol{B}^{+}{}_n\boldsymbol{B}_m v(t)\right) \\ &= \boldsymbol{A}_m\boldsymbol{e}(t) + \boldsymbol{B}_n\boldsymbol{B}^{+}{}_n\boldsymbol{B}_m v(t) \\ &= \boldsymbol{A}_m\boldsymbol{e}(t) + \boldsymbol{B}_m v(t). \end{aligned} \tag{32}$$

Equations. (32) is given only by the matrices $\boldsymbol{A}_m$ and $\boldsymbol{B}_m$ of the model. The augmented system can be derived from Eqs. (21) and (32) as follows:

$$\dot{\hat{\boldsymbol{e}}}(t) = \boldsymbol{A}_{eb}\hat{\boldsymbol{e}}(t) + \boldsymbol{B}_{eb}v(t), \tag{33}$$

where

$$\boldsymbol{A}_{eb} = \begin{bmatrix} \boldsymbol{A}_m & \boldsymbol{0} \\ \boldsymbol{C}_m & 0 \end{bmatrix},$$

$$\boldsymbol{B}_{eb} = \begin{bmatrix} \boldsymbol{B}_m \\ 0 \end{bmatrix}, \hat{\boldsymbol{e}}(t) = \begin{bmatrix} \boldsymbol{e}(t) \\ \varepsilon(t) \end{bmatrix}.$$

It should be noted that the matrices $\boldsymbol{A}_{eb}$ and $\boldsymbol{B}_{eb}$ are also determined by those of the model. The feedback gain, $\boldsymbol{F}_{1b} \in \mathbb{R}^{1\times n}$, and the feedforward gain, $\boldsymbol{F}_{2b} \in \mathbb{R}^{1\times 1}$, are obtained by Eqs. (23)–(25). Thus,   is given as follows:

$$v(t) = \boldsymbol{F}_{1b}\boldsymbol{e}(t) + \boldsymbol{F}_{2b}\int \left(y(t) - y_m(t) \right) dt. \quad (34)$$

From Eqs. (30) and (34), the plant input is obtained as follows:

$$u(t) = \boldsymbol{K}_{1b}\boldsymbol{x}(t) + \boldsymbol{K}_{2b}r(t) + \boldsymbol{B}_f \left\{ \boldsymbol{F}_{1b}\boldsymbol{e}(t) + \boldsymbol{F}_{2b}\int \left(y(t) - y_m(t) \right) dt \right\}. \quad (35)$$

4.2. MIMO System

In Eq. (13), the matrices $\boldsymbol{A}_m$, $\boldsymbol{B}_m$, and $\boldsymbol{C}_m$ are defined as follows:

$$\begin{cases} \boldsymbol{A}_m = \begin{bmatrix} \tilde{\boldsymbol{A}}_1 & 0 & \cdots & 0 \\ 0 & \tilde{\boldsymbol{A}}_2 & \ddots & \vdots \\ \vdots & \ddots & \ddots & 0 \\ 0 & \cdots & 0 & \tilde{\boldsymbol{A}}_k \end{bmatrix} \in \mathbb{R}^{n\times n}, \boldsymbol{B}_m = \begin{bmatrix} \tilde{\boldsymbol{B}}_1 & 0 & \cdots & 0 \\ 0 & \tilde{\boldsymbol{B}}_2 & \ddots & \vdots \\ \vdots & \ddots & \ddots & 0 \\ 0 & \cdots & 0 & \tilde{\boldsymbol{B}}_p \end{bmatrix} \in \mathbb{R}^{n\times p}, \\ \boldsymbol{C}_m = \begin{bmatrix} \tilde{\boldsymbol{C}}_1 & 0 & \cdots & 0 \\ 0 & \tilde{\boldsymbol{C}}_2 & \ddots & \vdots \\ \vdots & \ddots & \ddots & 0 \\ 0 & \cdots & 0 & \tilde{\boldsymbol{C}}_q \end{bmatrix} \in \mathbb{R}^{q\times n}, \end{cases}$$

where $\tilde{\boldsymbol{A}}_i \in \mathbb{R}^{l\times l}$, $\tilde{\boldsymbol{B}}_i \in \mathbb{R}^{l\times 1}$, and $\tilde{\boldsymbol{C}}_i \in \mathbb{R}^{1\times l}$ are described by

$$\tilde{\boldsymbol{A}}_i = \begin{bmatrix} 0 & 1 & 0 & \cdots & 0 \\ \vdots & 0 & 1 & \ddots & \vdots \\ \vdots & & \ddots & \ddots & 0 \\ 0 & \cdots & \cdots & 0 & 1 \\ \tilde{a}_{i1} & \tilde{a}_{i2} & \cdots & \tilde{a}_{i(l-1)} & \tilde{a}_{il} \end{bmatrix} \; (i = 1, 2, \cdots, k),$$

$$\tilde{\boldsymbol{B}}_i = \begin{bmatrix} 0 & \cdots & 0 & \tilde{b}_i \end{bmatrix}^T \; (i = 1, 2, \cdots, p),$$

$$\tilde{\boldsymbol{C}}_i = \begin{bmatrix} 1 & 0 & \cdots & 0 \end{bmatrix} \; (i = 1, 2, \cdots, q).$$

where it is assumed that $n = l \times k$ and $k \geq p, q$. To apply the model-following control described in Section 2 to the normalized MIMO plant, Eqs. (17) and (18) are given as follows:

$$\begin{aligned} \boldsymbol{K}_{1b} &= \boldsymbol{B}_n^{+}\left(\boldsymbol{A}_m - \boldsymbol{A}_n \right) \\ &= \begin{bmatrix} \tilde{\boldsymbol{K}}_1 & \boldsymbol{0} & \cdots & \boldsymbol{0} \\ \boldsymbol{0} & \tilde{\boldsymbol{K}}_2 & \ddots & \vdots \\ \vdots & & \ddots & \boldsymbol{0} \\ \boldsymbol{0} & \cdots & \boldsymbol{0} & \tilde{\boldsymbol{K}}_k \end{bmatrix} \end{aligned} \quad (36)$$

and

$$K_{2b} = \left(-C_m A_m^{-1} B_n\right)^{-1} = \begin{bmatrix} \tilde{a}_{11} & 0 & \cdots & 0 \\ 0 & \tilde{a}_{21} & \ddots & \vdots \\ \vdots & \ddots & \ddots & 0 \\ 0 & \cdots & 0 & \tilde{a}_{q1} \end{bmatrix} \quad (37)$$

where

$$\tilde{K}_i = \left[\tilde{a}_{i1} \quad \tilde{a}_{i2} \quad \cdots \quad \tilde{a}_{i(l-1)} \quad \tilde{a}_{il}\right]. \quad (37)$$

Equations. (36) and (37) are also parameterized only by model parameters, $\tilde{a}_{il}$. On the other hand, the argument system for MIMO is obtained by the same procedure as that described in Section 4.1 as follows:

$$\dot{\hat{e}}(t) = A_{eb}\hat{e}(t) + B_{eb}v(t), \quad (38)$$

where

$$A_{eb} = \begin{bmatrix} A_m & \mathbf{0} \\ C_m & 0 \end{bmatrix},$$

$$B_{eb} = \begin{bmatrix} B_m \\ \mathbf{0} \end{bmatrix}, \hat{e}(t) = \begin{bmatrix} e(t) \\ \varepsilon(t) \end{bmatrix}.$$

The matrices A_{eb} and B_{eb} are determined by those of the model. Furthermore, the plant input $u(t)$ is obtained as follows:

$$u(t) = K_{1b}x(t) + K_{2b}r(t) + B_f\left\{F_{1b}e(t) + F_{2b}\int\left(y(t) - y_m(t)\right)dt\right\}. \quad (39)$$

Figure 3 shows a block diagram of the proposed method.

To improve the robustness against parameter variations, the following equation is defined:

$$u(t) = K_{1b}x(t) + K_{2b}r(t) + B_f\left\{F_{1b}e(t) + F_{2b}\int\left(y(t) - y_m(t)\right)dt\right\}. \quad (40)$$

where α is a parameter compensator. By increasing α , the system becomes decouplable and robust to parameter variations, as shown in Section 5. The theoretical analysis of the effectiveness by increasing α would be investigated in the future.

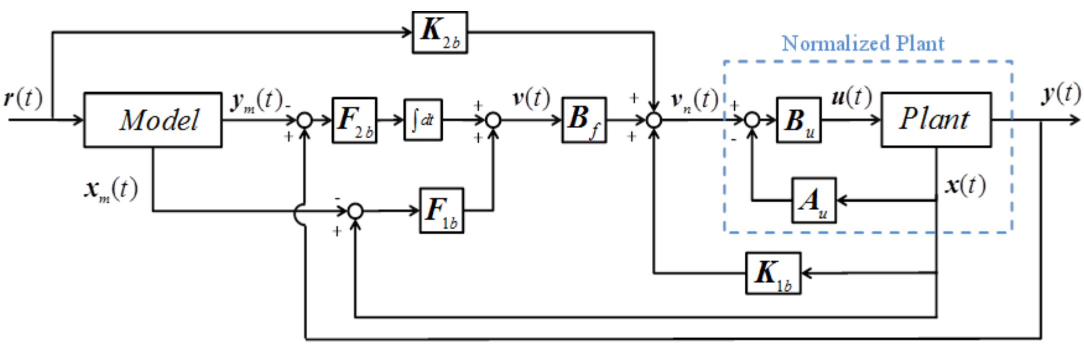

Figure 3. The Block Diagram Of The Proposed Method

5. Simulation Results

In this section, the effectiveness of the proposed method is shown by the results of a simulation. The control system is simulated using MATLAB/Simulink.

5.1. SISO Plant

In the simulation, a SISO plant is used, and described by

$$\begin{cases} \dot{\boldsymbol{x}}(t) = \begin{bmatrix} 0 & 1 \\ -a_1 & -a_2 \end{bmatrix} \boldsymbol{x}(t) + \begin{bmatrix} b_1 \\ b_2 \end{bmatrix} u(t) \\ y(t) = \begin{bmatrix} 1 & 0 \end{bmatrix} \boldsymbol{x}(t) \end{cases}, \tag{41}$$

where $a_1 = 2$, $a_2 = 2$, $b_1 = 1$, and $b_2 = -1$. The SISO model is set to

$$\begin{cases} \dot{\boldsymbol{x}}_m(t) = \begin{bmatrix} 0 & 1 \\ -\omega_n^2 & -2\zeta\omega_n \end{bmatrix} \boldsymbol{x}_m(t) + \begin{bmatrix} 0 \\ \omega_n^2 \end{bmatrix} r(t) \\ y_m(t) = \begin{bmatrix} 1 & 0 \end{bmatrix} \boldsymbol{x}_m(t) \end{cases}, \tag{42}$$

where $\omega_n = 10.0$ and $\zeta = 0.7$. The model input, $r(t)$, is a step signal of magnitude 1. The weight matrix $\boldsymbol{Q}$, $\boldsymbol{R}$ for the optimal control method and other gain parameters are listed in Table 1.

An input-side step disturbance of magnitude –0.1 is applied at time $t = 2.0$. To investigate the robustness, the modeling error for the plant is set to be ±50% for the coefficient . The simulation result by the proposed method are shown Fig 4. Therefore, the proposed method is robust to parameter variations.

Table 1. The Parameters (SISO Plant)

Parameter	Value
$\boldsymbol{K}_{1a}, \boldsymbol{K}_{1b}$	$[-0.2945 \quad -0.0095], [-100 \quad -14]$
$\boldsymbol{K}_{2a}, \boldsymbol{K}_{2b}$	0.2945, 100
$\boldsymbol{Q}$	$\begin{bmatrix} 10^6 & 0 & 0 \\ 0 & 10^6 & 0 \\ 0 & 0 & 10^6 \end{bmatrix}$
$\boldsymbol{R}$	1
$\boldsymbol{F}_{1a}, \boldsymbol{F}_{1b}$	$[-1.7318 \quad -1.0000], [-1.7311 \quad -0.9999]$
$\boldsymbol{F}_{2a}, \boldsymbol{F}_{2b}$	$-1000, -1000$

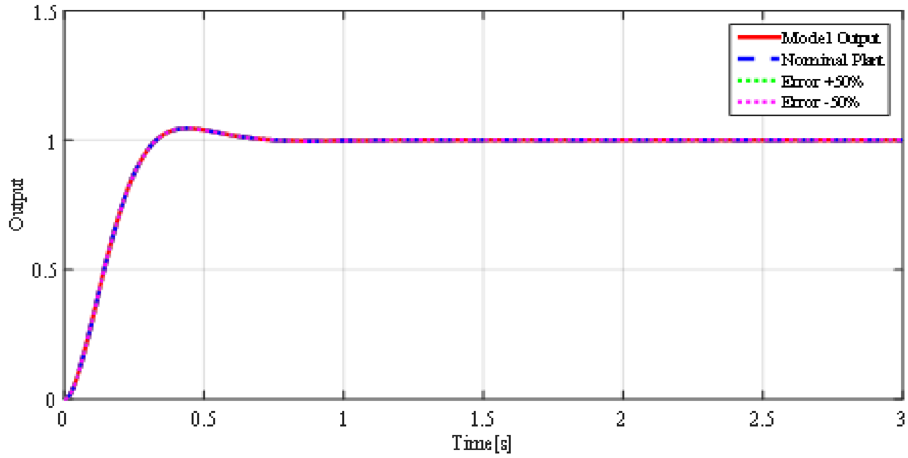

Figure 4. Simulation Result of the Proposed Method Of SISO Systems

5.2. Decoupled Plant for a MIMO System

An example of the decoupled MIMO plant used in this simulation is described as follows:

$$\begin{cases} \dot{\boldsymbol{x}}(t) = \boldsymbol{A}\boldsymbol{x}(t) + \boldsymbol{B}\boldsymbol{u}(t) \\ \quad = \begin{bmatrix} 0 & 1 & 0 & 0 \\ -a_{11} & -a_{12} & 0 & 0 \\ 0 & 0 & 0 & 1 \\ 0 & 0 & -a_{21} & -a_{22} \end{bmatrix} \boldsymbol{x}(t) + \begin{bmatrix} 0 & 0 \\ b_{11} & 0 \\ 0 & 0 \\ 0 & b_{22} \end{bmatrix} \boldsymbol{u}(t) \\ \boldsymbol{y}(t) = \begin{bmatrix} 1 & 0 & 0 & 0 \\ 0 & 0 & 1 & 0 \end{bmatrix} \boldsymbol{x}(t) \end{cases}, \tag{43}$$

where

$$a_{11} = \frac{212.6789}{0.135}, a_{12} = \frac{0.567}{0.135}, b_{11} = \frac{2.1632}{0.135},$$
$$a_{21} = \frac{42.6293}{0.135}, a_{22} = \frac{0.567}{0.135}, b_{22} = \frac{1.2858}{0.135}.$$

The MIMO model is set to

$$\begin{cases} \dot{\boldsymbol{x}}_m(t) = \begin{bmatrix} 0 & 1 & 0 & 0 \\ -\omega_1^2 & -2\zeta_1\omega_1 & 0 & 0 \\ 0 & 0 & 0 & 1 \\ 0 & 0 & -\omega_2^2 & -2\zeta_2\omega_2 \end{bmatrix} \boldsymbol{x}_m(t) + \begin{bmatrix} 0 & 0 \\ \omega_1^2 & 0 \\ 0 & 0 \\ 0 & \omega_2^2 \end{bmatrix} \boldsymbol{r}(t) \\ \boldsymbol{y}_m(t) = \begin{bmatrix} 1 & 0 & 0 & 0 \\ 0 & 0 & 1 & 0 \end{bmatrix} \boldsymbol{x}_m(t) \end{cases}, \tag{44}$$

where $\omega_1 = 20.0$, $\zeta_1 = 0.7$, $\omega_2 = 10.0$, and $\zeta_2 = 0.7$. The model input, $\boldsymbol{r}(t)$, consists of the step signal and the sine wave:

$$\boldsymbol{r}(t) = \begin{bmatrix} r_1(t) \\ r_2(t) \end{bmatrix} = \begin{bmatrix} 1 \\ 100\sin 10t \end{bmatrix}. \tag{45}$$

For the optimal control method, the weight matrices $\boldsymbol{Q}$ and $\boldsymbol{R}$ are set as listed in Table 2. The gain parameters are listed in the same Table.

Table 2. The Parameters (Decoupled Plant of a MIMO System)

Parameter	Value
$\boldsymbol{K}_{1a}, \boldsymbol{K}_{1b}$	$\begin{bmatrix} 92.1576 & -0.6121 & -0.4343 & 0.0495 \\ -4.1218 & 0.0252 & -75.1332 & -2.5009 \end{bmatrix}$, $\begin{bmatrix} -100 & -14 & 0 & 0 \\ 0 & 0 & -400 & -28 \end{bmatrix}$
$\boldsymbol{K}_{2a}, \boldsymbol{K}_{2b}$	$\begin{bmatrix} 6.2458 & -0.8316 \\ -0.2575 & 42.0315 \end{bmatrix}$, $\begin{bmatrix} 100 & 0 \\ 0 & 400 \end{bmatrix}$
$\boldsymbol{Q}$	$diag\begin{bmatrix} 10^6 & 10^6 & 10^6 & 10^6 & 10^6 & 10^6 \end{bmatrix}$
$\boldsymbol{R}$	$\begin{bmatrix} 1 & 0 \\ 0 & 1 \end{bmatrix}$

$\boldsymbol{F}_{1a}, \boldsymbol{F}_{1b}$	$10^3\begin{bmatrix} -1.7259 & -0.9992 & -0.0059 & -0.0030 \\ 0.0048 & 0.0029 & -1.6906 & -0.9972 \end{bmatrix}$, $10^3\begin{bmatrix} -1.7311 & -0.9999 & 0 & 0 \\ 0 & 0 & -1.7311 & -0.9999 \end{bmatrix}$
$\boldsymbol{F}_{2a}, \boldsymbol{F}_{2b}$	$-1000, -1000$

An input-side step disturbance of magnitude -0.1 is applied at time $t = 2.0$. To show the robustness, the modeling error for the plant is set to be ±50% for the coefficients $a_{11}, a_{12}, a_{21}, a_{22}$. The simulation results for the output responses, y_1 and y_2, of the conventional method are shown in Figs. 5 and 6. The simulation results for the output responses, y_1 and y_2, of the proposed method are shown in Figs. 7 and 8. As can be seen, the steady state error occurs in the conventional method when there is modeling error for plants of the MIMO system. In contrast, the proposed method is robust to parameter variations.

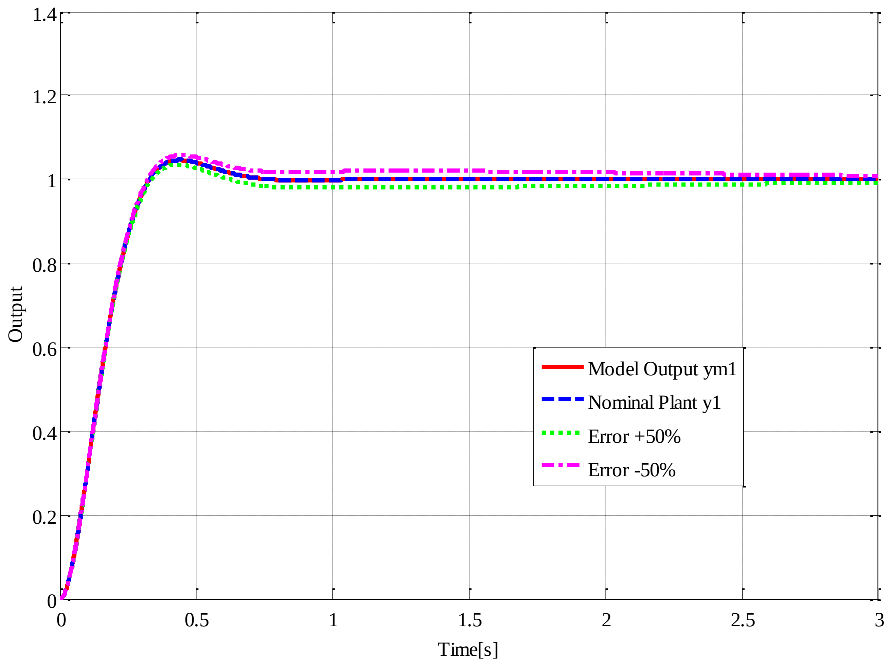

Figure 5. The Output Responses, Y_1, of the Conventional Method of the MIMO System

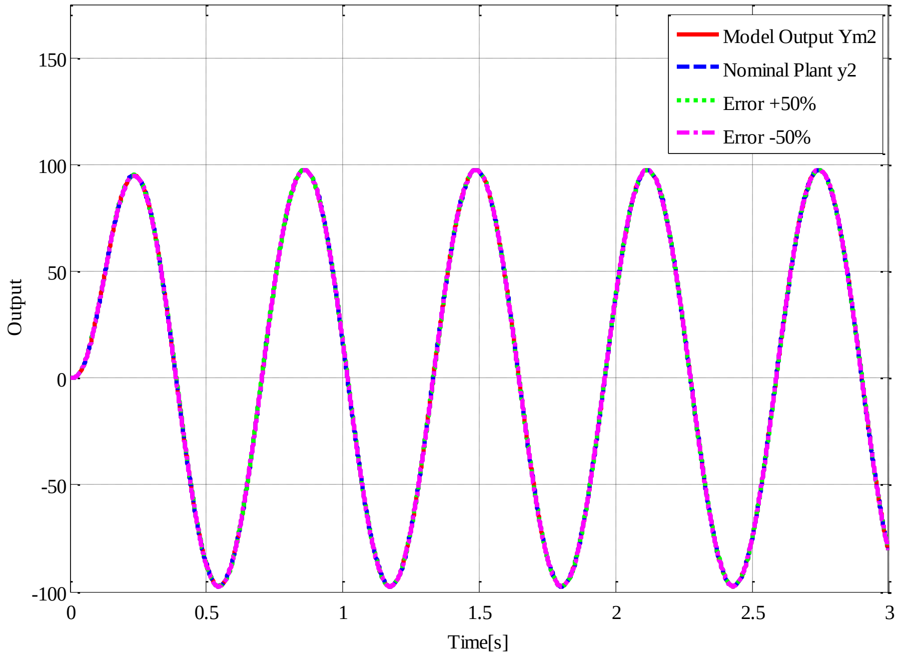

Figure 6. The Output Responses, Y_2, Of The Conventional Method Of The MIMO System

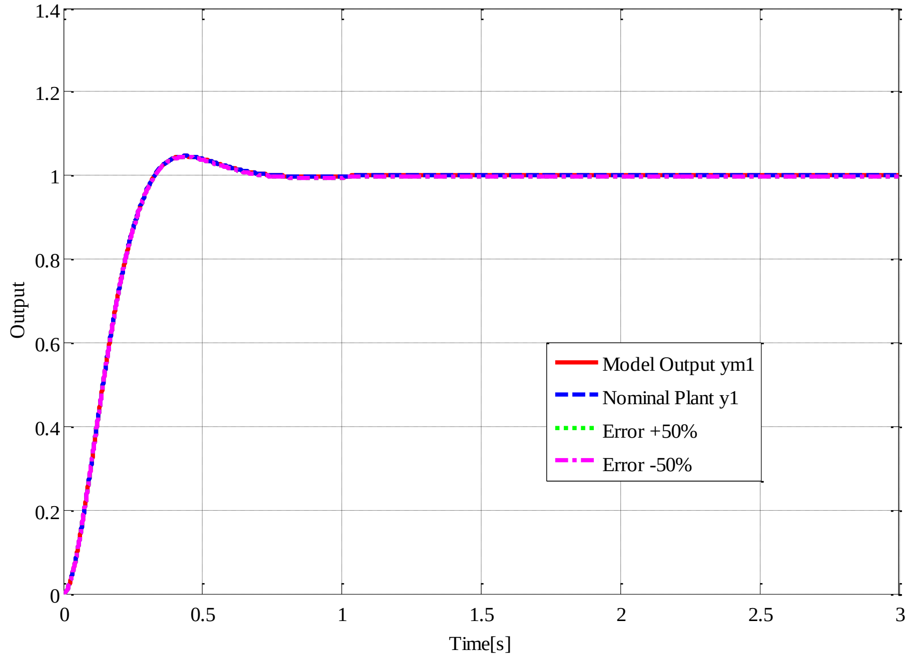

Figure 7. The Output Responses, Y_1, Of The Proposed Method of the MIMO System

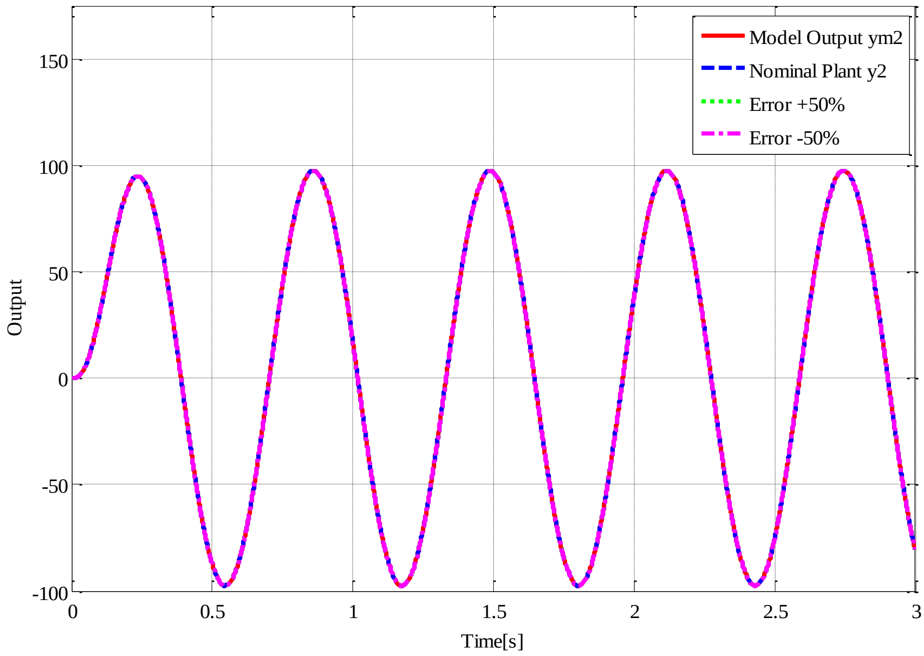

Figure 8. The Output Responses, Y_2, of the Proposed Method of the MIMO System

5.3. Decoupled Plant for a MIMO System

An example of the decoupled MIMO plant used in this simulation is described as follows:

$$\begin{cases} \dot{\boldsymbol{x}}(t) = \boldsymbol{A}\boldsymbol{x}(t) + \boldsymbol{B}\boldsymbol{u}(t) \\ \quad = \begin{bmatrix} 0 & 1 & 0 & 0 \\ -a_{11} & -a_{12} & -a_{13} & -a_{14} \\ 0 & 0 & 0 & 1 \\ -a_{21} & -a_{22} & -a_{23} & -a_{24} \end{bmatrix} \boldsymbol{x}(t) + \begin{bmatrix} 0 & 0 \\ b_{11} & b_{12} \\ 0 & 0 \\ b_{21} & b_{22} \end{bmatrix} \boldsymbol{u}(t), \\ \boldsymbol{y}(t) = \begin{bmatrix} 1 & 0 & 0 & 0 \\ 0 & 0 & 1 & 0 \end{bmatrix} \boldsymbol{x}(t) \end{cases} \tag{46}$$

where

$$a_{11} = \frac{212.6789}{0.135}, a_{12} = \frac{0.567}{0.135}, a_{13} = -\frac{4.1552}{0.135}, a_{14} = 0,$$
$$b_{11} = \frac{2.1632}{0.135}, b_{12} = \frac{0.0428}{0.135},$$
$$a_{21} = -\frac{4.1552}{0.135}, a_{22} = 0, a_{23} = \frac{42.6293}{0.135}, a_{24} = \frac{0.567}{0.135},$$
$$b_{21} = \frac{0.0530}{0.135}, b_{22} = \frac{1.2858}{0.135}.$$

The same MIMO model and the same model input, $\boldsymbol{r}(t)$, as those in Section 5.2 are used. For the optimal control method, the weight matrices $\boldsymbol{Q}$ and $\boldsymbol{R}$ are set as listed in Table 3. The gain parameters are listed in the same Table.

An input-side step disturbance of magnitude -0.1 is applied at time $t = 0.2$ .To show the robustness, the modeling error for the plant is set to ±50% for the coefficients

$a_{11} \cdots a_{14}, a_{21} \cdots a_{24}$. The simulation results for the output responses, y_1 and y_2, of the conventional method are shown in Figs. 9 and 10. A parameter compensator, $\alpha = 1.0$, and the simulation results for the output responses, y_1 and y_2, of the proposed method are shown in Figs. 11 and 12, respectively. The modeling error for the plant is set to ±90% for the coefficients $a_{11} \cdots a_{14}, a_{21} \cdots a_{24}$, and the simulation results for the output responses, y_1 and y_2, of the proposed method are shown in Figs. 13 and 14, respectively. A parameter compensator, , and the simulation results for the output responses, and , of the proposed method are shown in Figs. 15 and 16, respectively. Figs. 13–14 show that decoupling is achieved in the proposed method. Figs. 15–16 show that the system becomes decouplable by increasing α when it has a large modeling error.

Table 3. The Parameters (Coupled Plant Of MIMO System)

Parameter	Value
$\boldsymbol{K}_{1a}, \boldsymbol{K}_{1b}$	$\begin{bmatrix} 92.1576 & -0.6121 & -0.4343 & 0.0495 \\ -4.1218 & 0.0252 & -75.1332 & -2.5009 \end{bmatrix}, \begin{bmatrix} -100 & -14 & 0 & 0 \\ 0 & 0 & -400 & -28 \end{bmatrix}$
$\boldsymbol{K}_{2a}, \boldsymbol{K}_{2b}$	$\begin{bmatrix} 6.2458 & -0.8316 \\ -0.2575 & 42.0315 \end{bmatrix}, \begin{bmatrix} 100 & 0 \\ 0 & 400 \end{bmatrix}$
$\boldsymbol{Q}$	$diag\begin{bmatrix} 10^6 & 10^6 & 10^6 & 10^6 & 10^6 & 10^6 \end{bmatrix}$
$\boldsymbol{R}$	$\begin{bmatrix} 1 & 0 \\ 0 & 1 \end{bmatrix}$
$\boldsymbol{F}_{1a}, \boldsymbol{F}_{1b}$	$10^3 \begin{bmatrix} -1.7259 & -0.9992 & -0.0059 & -0.0030 \\ 0.0048 & 0.0029 & -1.6906 & -0.9972 \end{bmatrix}, 10^3 \begin{bmatrix} -1.7311 & -0.9999 & 0 & 0 \\ 0 & 0 & -1.7311 & -0.9999 \end{bmatrix}$
$\boldsymbol{F}_{2a}, \boldsymbol{F}_{2b}$	$-1000, -1000$

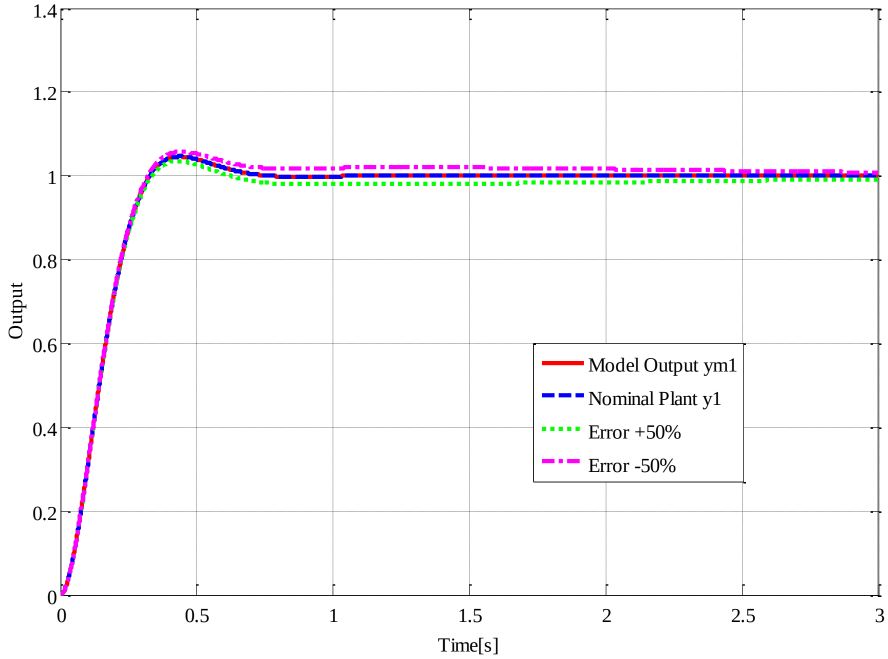

Figure 9. The Output Responses, y_1, of the Conventional Method of the Coupling System

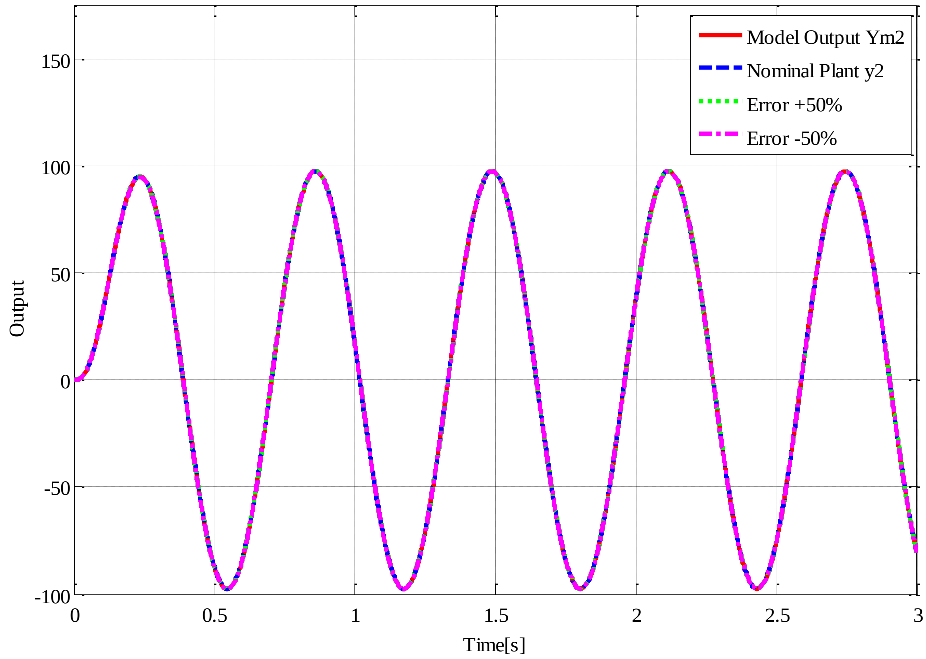

Figure 10. The Output Responses, Y_2, of the Conventional Method of the Coupling System

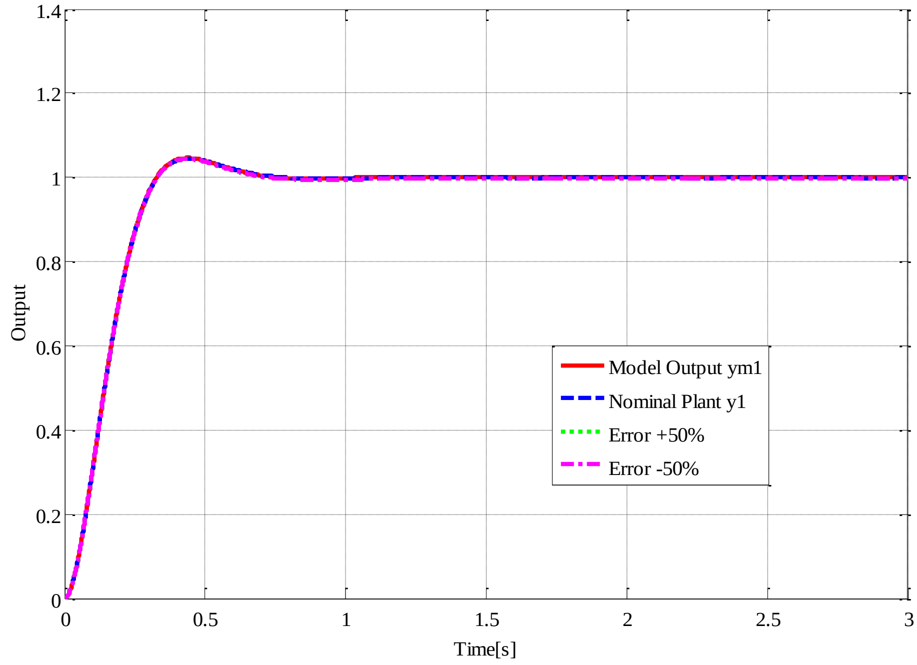

Figure 11. The Output Responses, Y_1, of the Proposed Method of the Coupling System

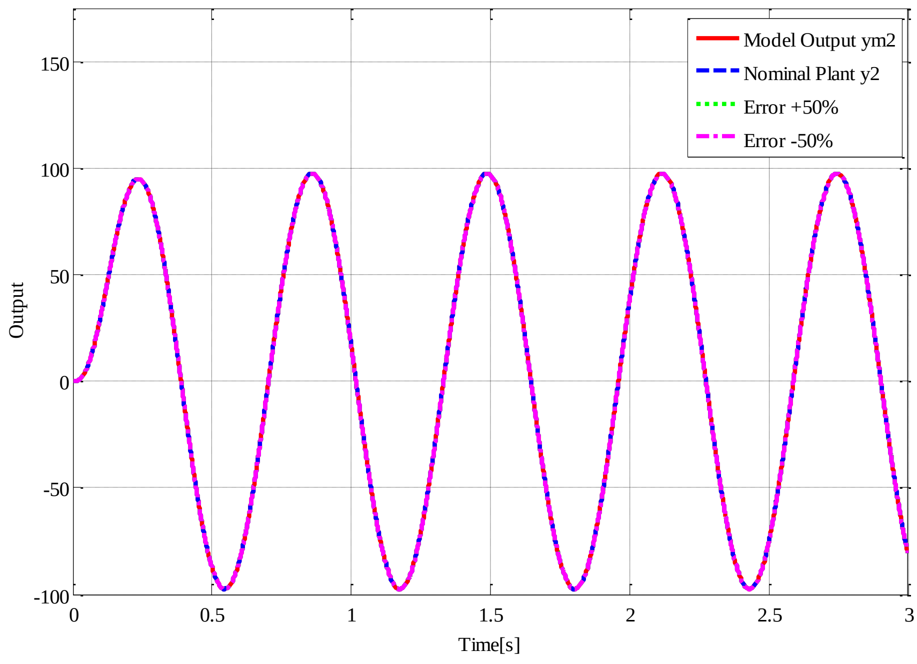

Figure 12. The Output Responses, Y_2, of the Proposed Method of the Coupling System

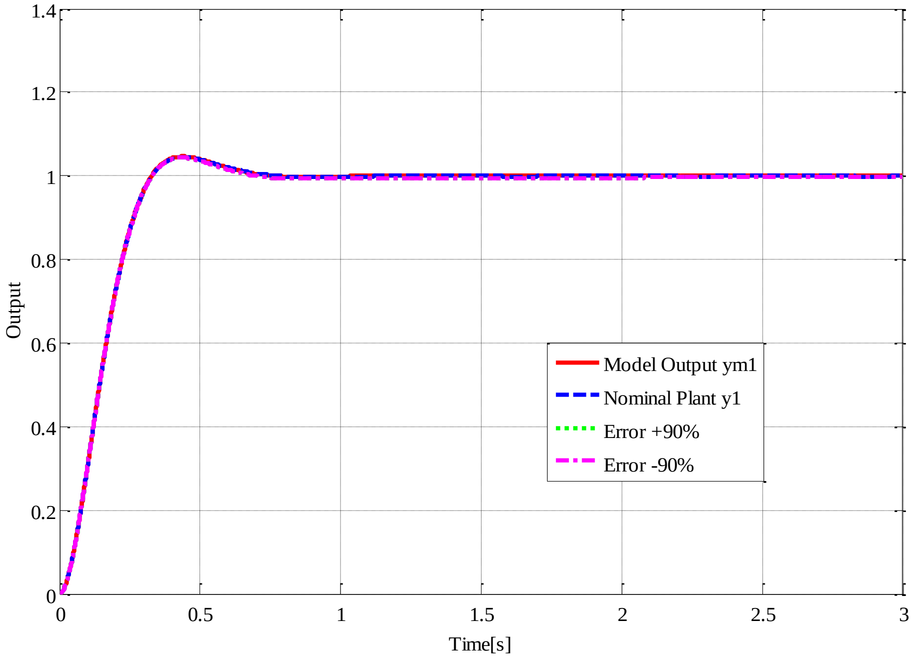

Figure 13. The Output Responses, Y_1,, of the Proposed Method of the Coupling System When the Modeling Error Is ±90%

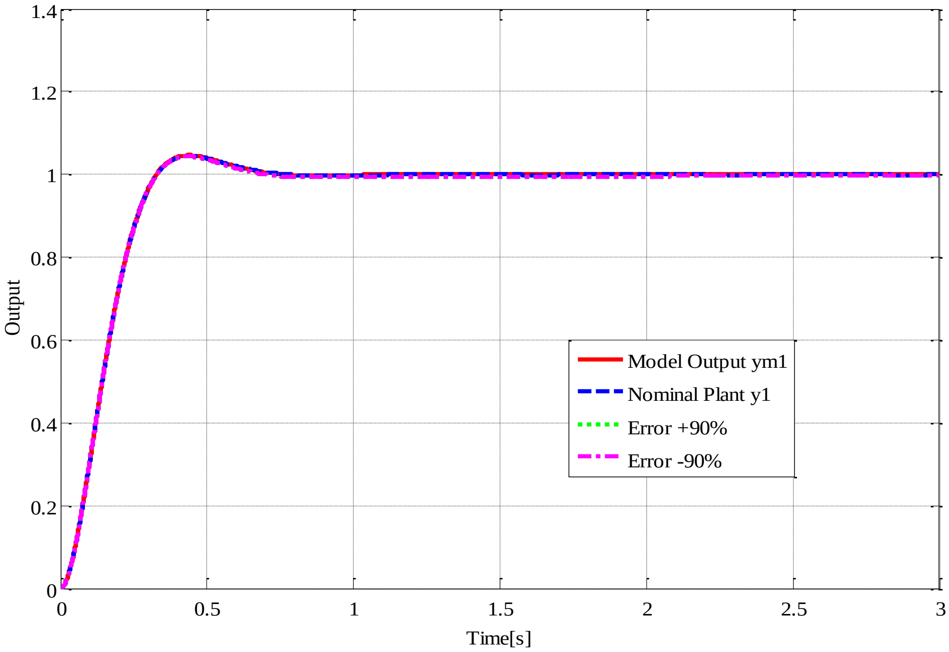

Figure 14. The Output Responses, Y_2,, of the Proposed Method of the Coupling System When the Modeling Error Is ±90%

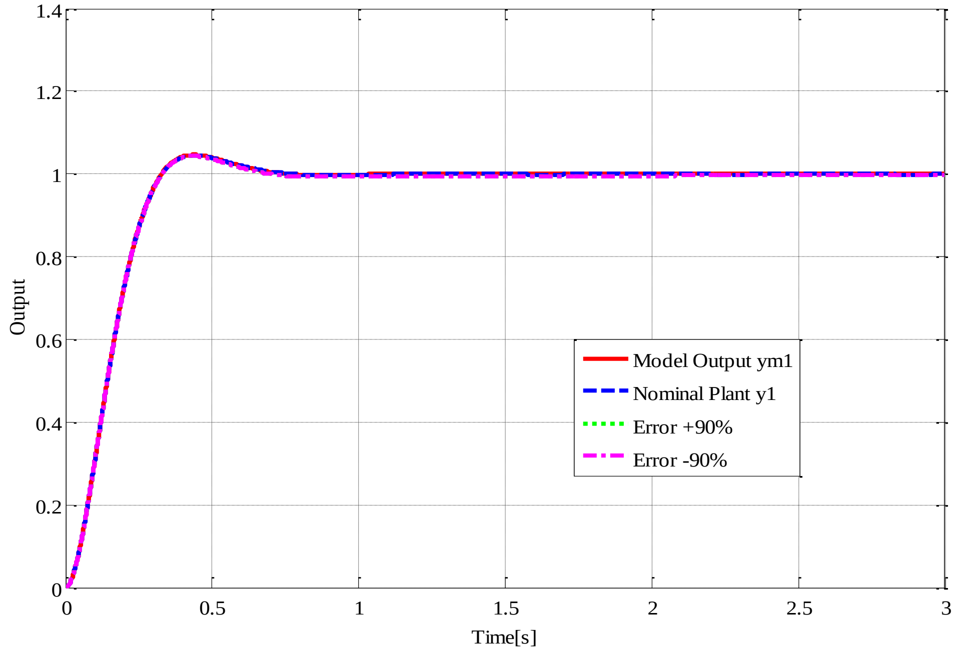

Figure 15. The Output Responses, Y_1,, of the Proposed Method of the Coupling System When the Modeling Error Is ±90% and α=10

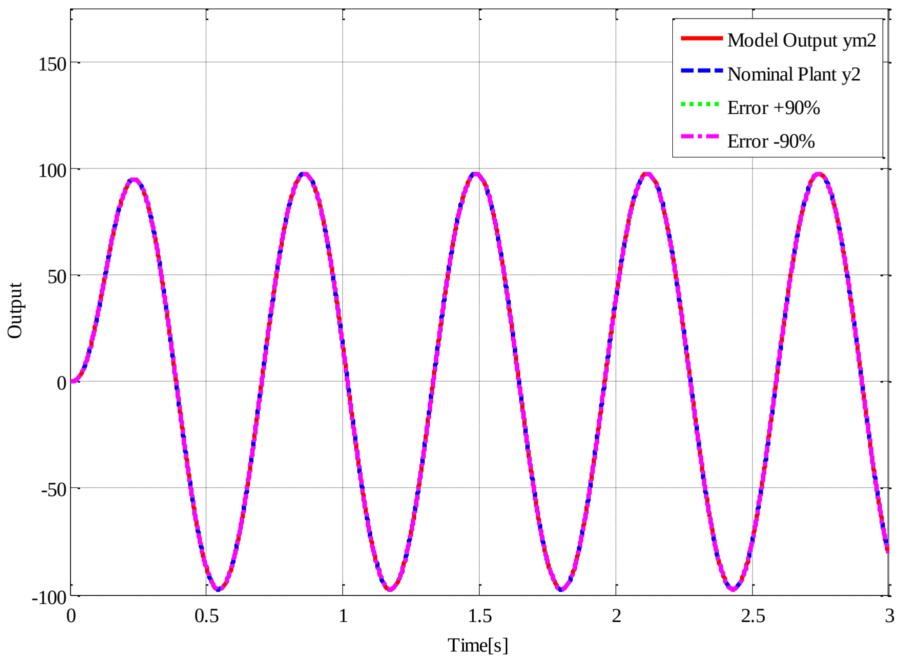

Figure 16. The Output Responses, Y_2,, of the Proposed Method of the Coupling System When the Modeling Error is ±90% and α=10

6. Experimental Study

In this section, we confirm the effectiveness of the proposed method by performing an experiment of positioning control with a DC motor [20]. In the industry, electric motors are used widely in products such as automated factory devices, robotics, and transport equipment.

There The experimental control system is shown in Figure 17 and consists of a DC motor, an encoder, a counter that measures the information from the encoder, a host PC that transmits the control information, a target PC that calculates the manipulated variable, and a D/A converter.

First, the control signal used to move the DC motor is transmitted from the host PC to the target PC and then to the D/A converter, which has a resolution of 12 bits. Next, the output of the motor is transformed into a pulse of phases A and B by the encoder, which has a resolution of 1.534×103 radians/count. The counter measures these pulses and transmits the positional signal to the host PC through the target PC. Figure 18 shows the DC motor used in the experimental study, which was made by PID Corporation (PID-QET ii). The motor is equipped with an inertial load disk that has a radius of 0.0248 m and a mass of 0.068 kg. The control plant is identified by the step response method as follows:

$$G(s) = \frac{b}{s^2 + as}, \tag{47}$$

where $a = 10.78$ and $b = 339.6$.

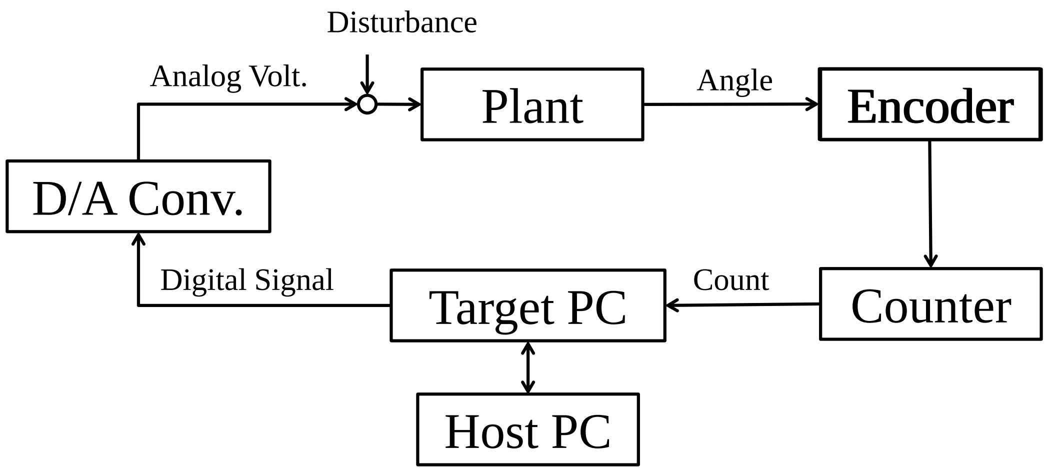

Figure 17. Motor Control System

Figure 18. DC Motor

6.1. SISO System

In this subsection, the effectiveness of the proposed method is shown by the experimental results with a SISO system. The target value r is set to 1 (180°). An input-side step disturbance of magnitude -0.1 is applied at $t=0.2$ s. In the experimental studies, the proposed method is applied to DC motors with masses of 0.1 kg and 0.2 kg. The weight matrix $\boldsymbol{Q}$, $\boldsymbol{R}$ with an optimal control method, and the gain parameters are obtained as listed in Table 1. The experimental results for the output response are shown in Figure 19. The effectiveness of the proposed method is confirmed by the experimental result to be about the same as the simulation predicted.

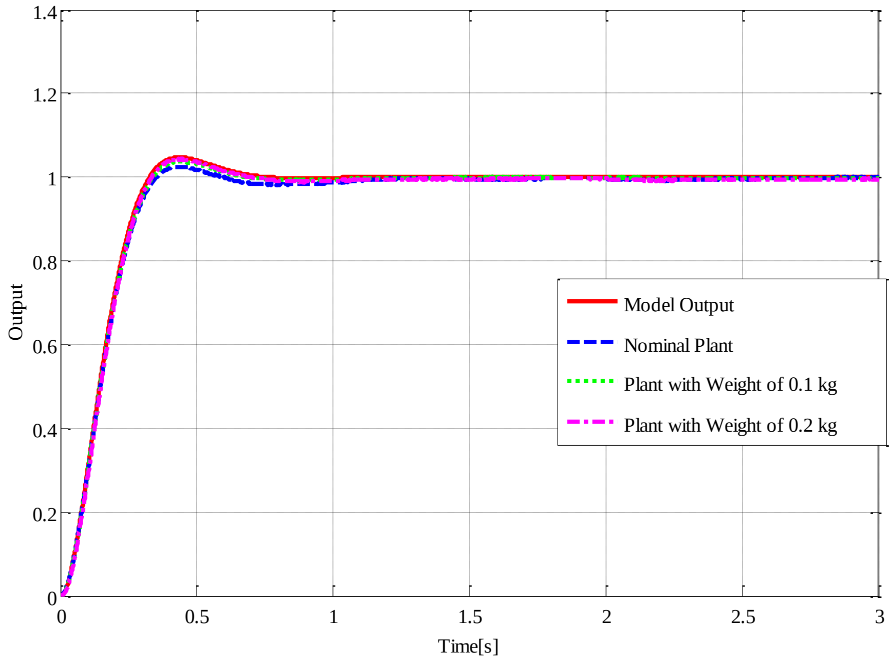

Figure 19. The Experimental Results for the Output Response

6.2. MIMO System

In this subsection, the effectiveness of the proposed method is shown by the experimental results with a MIMO system. A DC motor is virtually extended from the SISO system to the MIMO system because there is only SISO equipment available in the laboratory. As shown in Figure 20, a DC motor is part of the system. Control object 1 is a DC motor, and the transfer function of control object 2 is

$$\frac{K}{Ts+1}. \quad (48)$$

The gain parameters are

$$k_{11} = 1, k_{12} = 0.3, k_{21} = 0.1, k_{22} = 1, T = 0.5, K = 200.$$

The experimental results for the output response are shown in Figure 21. The effectiveness of the proposed method is confirmed by the experimental result to be about the same as predicted by the simulation.

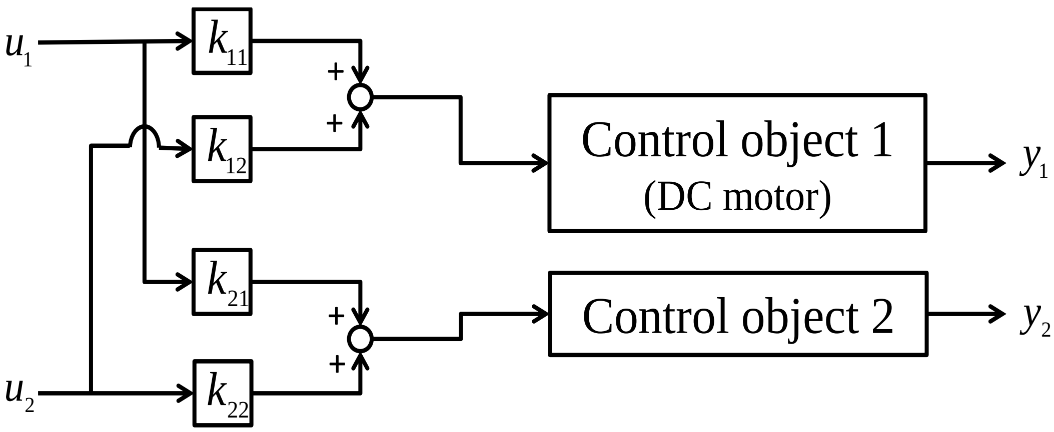

Figure 20. Structure of the 2-input-2-output System

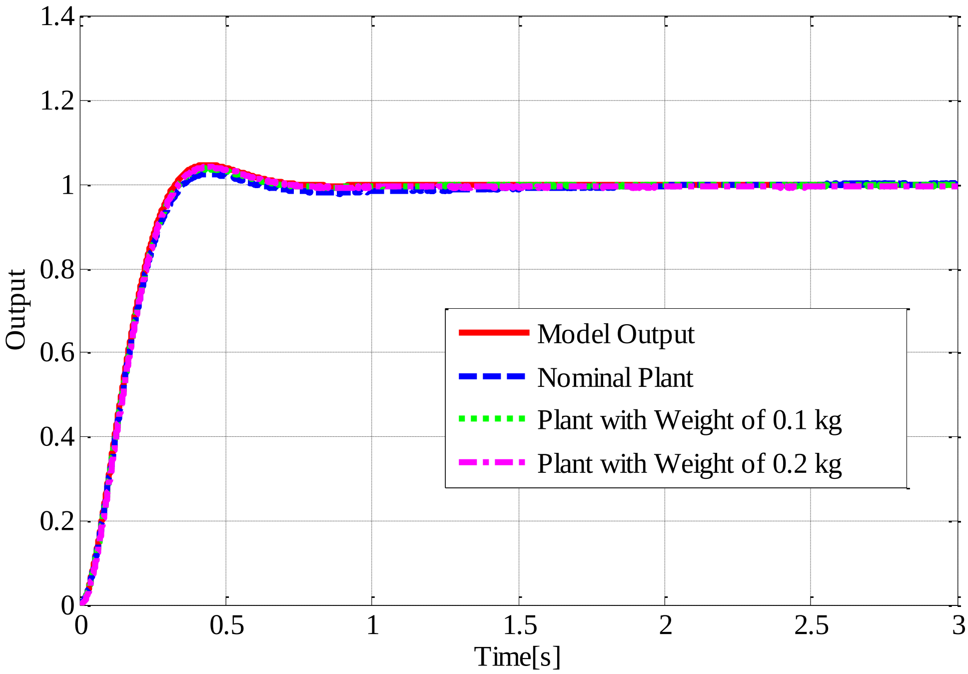

Figure 21. The Experimental Results for the Output Response, Y_1, of the MIMO System

7. Conclusions

In this paper, we have proposed a model-following control system design method that is independent of the plant parameters for SISO and MIMO systems. the normalized plant can be realized in case of the controlled plant with zero and the MIMO plant collectively. The proposed method can prevent the influence of an input-side disturbance and is robust against parameter changes. Furthermore, it becomes decouplable in the case of MIMO systems. The effectiveness of the proposed method has been confirmed by simulation studies in Section 5 and by the experimental results for positioning control with a DC motor in Section 6.

References

[1] Y. Fujisawa and M. Ikeda, "A Two-Degree-of-Freedom Design of Model Following Servosystems", Transactions of the Institute of Systems, Control and Information Engineers, vol. 7, issue 5, **(1994)**, pp. 185-191.

[2] D. Nakazawa, S. Suzuki, S. Sakai and K. Nonami, "Formation Flight Control of Small Unmanned Helicopters", Transactions of the The Japan Society of Mechanical Engineers, vol. 74, issue 747, **(2008)**, pp.2737-2746.

[3] D. Xinmin, X. Zhiguo and L. Qin, "Gain scheduled model following control of flight control system based on neural network", Proceedings of the IEEE international conference on neural networks & signal processing, vol. 1, **(2003)**, pp. 301-305.

[4] Furuta, Katsuhisa, and K. Katsumi, "Design of model-following servo controller", Automatic Control, IEEE Transactions on, vol. 27, issue. 3, **(1982)**, pp. 725-727.

[5] Y. Zhi-jun, QI. Xiao-hui and S. Gan-lin, "Model-following sliding mode controller design for flight control systems with wind disturbances", IEEE conference on industrial electronics and applications, **(2009)**, pp. 287-291.

[6] A. Tesfaye and M. Tomizuka, "Robust MIMO model following with application to trajectory motion control of robot arms", Proceedings of the 33rd conference on design and control, **(1994)**, pp. 814-819.

[7] A. Balestrino, G. De Maria and L. Sciavicco, "Hyperstable adaptive model following control of nonlinear plants", vol, 1, issue, 4, **(1982)**, pp. 232-236.

[8] KD. Young, "Variable structure model following control design for robotics applications", IEEE Journal on robotics and automation, vol, 4, issue, 5, **(1988)**, pp. 556-61.

[9] D. Nakazawa, S. Suzuki, S. Sakai and K. Nonami, "Trajectory Following Control of Small-Scale Unmanned Helicopter by Using Model-Following-Type Model Predictive Control", Transactions of the JSME, vol, 74, issue 746, **(2008)**, pp. 2504-11.

[10] W. Wang, K. Nonami and Y. Ohira, "Model Reference Sliding Mode Control of Small Helicopter X.R.B based on Vision", International Journal of Advanced Robotic Systems, vol. 5, issue. 3, **(2008)**, pp. 235-42.

[11] N. Kobayashi and T. Nakamizo, "A Design of Dynamic Compensators for the Decoupling in Structural Aspects", The society of Instrument and Control Engineers, vol. 28, issue. 12, **(1992)**, pp. 1427-35.

[12] P. Wen and T-w. Lu, "Decoupling control of a twin rotor MIMO system using robust deadbeat control technique", IEE control theory and applications, vol. 2, issue. 11, **(2008)**, pp. 999-1007.

[13] L. Lan, K. Okabe, R. Oguro and H. Honda, "Decoupling control of 2-link manipulator with model following control and Proposed Control Gains Design (ICCAS 2012)", international conference on control automation and system, **(2012)**, pp. 1049-54.

[14] KJ. Astrom, KH. Johansson and QG. Wang, "Design of decoupled PI controllers for two-by-two systems", IEE Proc. Control theory, vol. 149, issue. 1, **(2002)**, pp. 74-81.

[15] Y. Asagi, K. Watanabe, E. Muramatsu and Y. Ariga, "Systematic Design Method of Decoupling of Non-minimum Phase Systems by State Feedback and Inverse System", The society of Instrument and Control Engineers, vol. 41, issue. 3, **(2005)**, pp. 234-41.

[16] Y. Zhang, L. Shien, C. Akujuobi and W. Ali, "Digital PID controller design for delayed multivariable systems", Asian Journal of Control, vol. 6, issue. 4, **(2004)**, pp. 483-95.

[17] J. Lee, DH. Kim and TF. Edgar, "Static decouplers for control of multivariable processes", AIChE Journal, vol. 51, issue. 10, **(2005)**, pp. 2712-20.

[18] D. Chen and DE. Seborg, "Multiloop PI/PID controller design based on gershgorin bands", Proceedings of the American Control Conference, **(2001)**, pp. 4122-27.

[19] K. Sakai, H. Shibasaki, R. Tanaka, T. Murakami and Y. Ishida, "A Design of a Robust Discrete-Time Controller", ISA Transactions, vol. 56, **(2015)**, pp.155-164.

[20] R. Tanaka, H. Shibasaki, O. Hiromitsu, T. Murakami and Y. Ishida, "Controller design approach based on linear programming", ISA Transactions, vol. 52, issue. 6, **(2013)**, pp. 744-51.

Authors

Shota Inou, he received the B.E. degree in Electronics and bioinformatics from Meiji University, Kawasaki, Japan, in 2014. He is currently studying toward the M.E. degree at Graduate School of Science and Technology, Meiji University. His research interests include continuous and digital control and its industrial applications

Yoshihisa Ishida, he received the B.E., M.E., and Dr.Eng. degrees in Electrical Engineering, Meiji University, Kawasaki, Japan, in 1970, 1972, and 1978, respectively. In 1975 he joined the Department of Electrical Engineering, Meiji University, as a research Assistant and became a Lecturer and an Associate Professor in 1978 and 1981, respectively. He is currently a Professor at the Department of Electronics and Bioinformatics, Meiji University. His current research interests include signal processing, speech analysis and recognition, and digital control. He is a member of the IEEE, and the IEICE of Japan.

